



Amino Acids as Environmentally-Friendly Corrosion Inhibitors for 2024 Aluminium Alloy in Alkaline Medium

Wisal A. Isa

Zainab W. Ahmed

Dept. of Chemistry/ College of Education for Pure Sciences (Ibn-Al-Haitham)/
University of Baghdad

Received in:24/May/2015,Accepted in:23/June/2015

Abstract

The corrosion behavior of 2024 aluminium alloy was investigated in alkaline medium (pH=13) containing $0.6 \text{ mol. dm}^{-3} \text{ NaCl}$ in absence and presence of different concentrations of three amino acids separately [Methionine, Glutamic acid and Lysine] as environmentally friendly corrosion inhibitors over the temperature range (293-308)K. Electrochemical polarization method using potentiostatic technique was employed. The inhibition efficiency increased with an increase of the inhibitor concentration but decreased with increase in temperature. The maximum efficiency value was found with lysine =80.4 of 293 k and $10^{-2} \text{ mol. dm}^{-3}$ concentration of lysine.

The adsorption of the amino acids was found to obey Langmuir adsorption isotherm. Some thermodynamic parameter (ΔG_{ads}) and activation energy (E^*) were calculated to demonstrate the mechanism of corrosion inhibition.

The kinetic parameters were calculated using Arrhenius theory. Suitable mechanism was proposed for the corrosion of 2024 aluminium alloy in alkaline medium. The polarization measurements indicated that the inhibitor is of mixed type.

The surface morphology of uninhibited and inhibited samples were investigated using optical microscope.

Key word: corrosion inhibition, 2024 alloy, Amino acids, Free energy of adsorption, Adsorption mechanism.

Introduction

Corrosion, which is an inevitable problem faced by almost all industries can be considered as one of the worst technical calamities of our time. Besides, from its direct costs in dollars, dollars, corrosion is a serious problem because it definitely contributes to the depletion of our natural resources.

Corrosion studies have also become important due to increasing awareness of the need to conserve the worlds metal resources[1]. Now-a-day more attention has been paid to control the metallic corrosion , due to increasing use of metals in all fields of technology:

Corrosion studies of aluminium and aluminium alloys have received considerable attention by researchers because of their wide industrial application and economic considerations[2]. Aluminium and aluminium alloys have emerged as alternate materials in aerospace and in some chemical processing industries. Due to their wide applications, they frequently come in contact with acids or bases during pickling, de-scaling, electrochemical etching and extensively used in chemical process industries. Most of the reported studies were conducted on corrosion of various metal and alloys in HCl and H_2SO_4 media[3,4,5].

Sodium hydroxide usually used for degreasing purpose as a part of our studies with corrosion behavior of aluminium and aluminium alloys in sodium hydroxide medium and corrosion control of the same using green inhibitors[6].

As corrosion inhibitors, various substances both inorganic and organic can be used. While organic inhibitors reduce the corrosion through film formation, organic compounds act mostly via adsorption processes on the metal surface and complex formation. As most efficient organic corrosion inhibitors could be toxic and thus unacceptable for the environment, contemporary studies are directed towards the search for alternative inhibitors that would be ecologically acceptable, stable non toxic and available at a relatively low cost, these compounds referred to as “green”, ‘eco-friendly”, or environmentally-friendly comprise both organic and inorganic inhibitors.

Among the organic inhibitors are bio-mimicking green inhibitors, such as amino acids, were conducted. Amino acids are completely soluble in aqueous media and can be produced with purity at low costs, in addition amino acids contain hetero atoms such as N,O and S (in some of them) which can form protective films [7].

The present work aims to characterize the effect of three amino acids (methionine, glutamic acid and lysine) as corrosion inhibitors for 2024 aluminium alloy in alkali medium (pH=13) containing (3.5% w/w) sodium chloride at temperature range (293-308)K. The three A.A. tested are L-enantiomers , methionine contains sulphur.

2. Experimental

2.1 Materials

Tested were performed on 2024 aluminium alloy specimen of the following composition given in Table (1).

2.2 Solution

Solution was prepared from analytical grade chemicals and doubly distilled water. Sodium hydroxide was obtained from fluka while methionine, lysine and glutamic acid were obtained from Aldrich chemical Co.Ltd. All measurements were performed in alkaline solution (pH=13) containing 3.5% $NaCl$ which have a comparable level to that of seawater. Double distilled water was used in all preparations.

2.3 Potentiostatic polarization measurements

The potentiostatic polarization measurements were performed in a conventional three-electrode glass cell with working volume 1000ml using Wenking M lab potentiostat. A working electrode was a sheet with circular shape (2 cm diameter and 2 mm thickness) which previously were grinded with emery papers of different graded (200,400,800,1200, and 2000) . Then they were polished mechanically with diamond paste using smooth cloth to surface mirror. The exposed surface area to the aggressive medium was 1cm².

A Pt counter electrode and silver – silver chloride as a reference electrode were used. Polarization measurements were performed at potentials from -200 mV to +200 mV at a scan rate of 2mV/s after steady state potential had been established in cathodic or anodic direction . All measurements were carried out in alkaline solution (pH=13) of 3.5% NaCl in the absence and presence of three different concentrations of the inhibitors.

The experimental result were reproducible and each experiment was carried out at least twice.

2.4 Optical microscopy measurements

The electrode surface of 2024 aluminium alloy was analyzed by optical microscope type were analyzed by optical microscope type of (Nikon Eclipse ME 600, Japan) before and after immersion in the aggressive solution in the absence and presence of the optimum concentration of the amino acid at 25°C. the specimens were washed gently with water, then dried carefully and examined without further treatments.

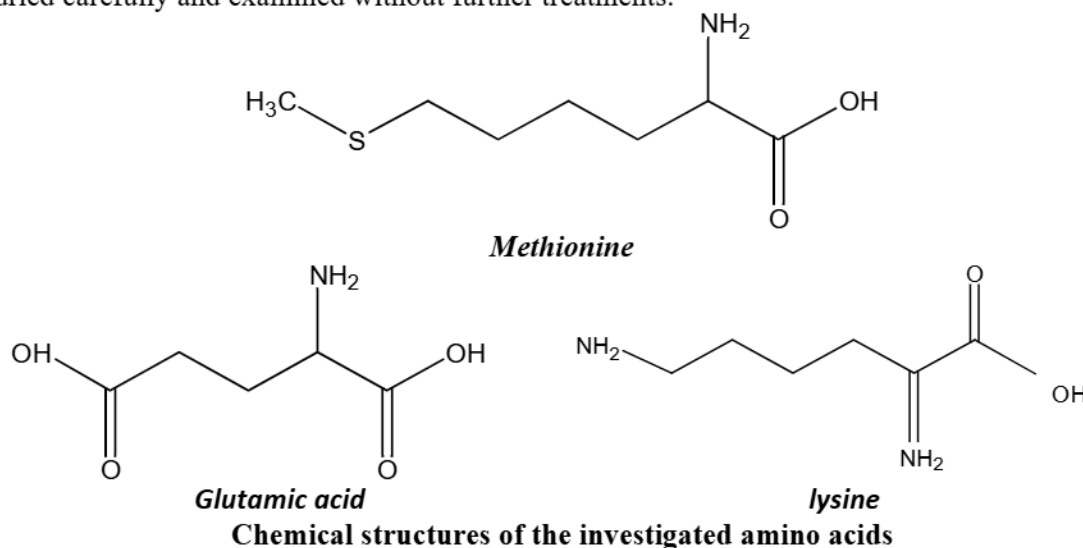


Figure (8) showed the images of Aluminium Alloy 2024 surface which immersed in the aggressive solution with and without the addition of 10⁻² mol. dm⁻³ of amine acids.

It can be observed that the specimen surface was strongly damaged in absence of inhibitor due to metal dissolution in the aggressive solution. A number of pits distributed over the surface are seen Figure (8 b).

However, no pits and cracks were observed in the micrograph after the addition of inhibitors to the aggressive solution Figure (8 c , 8 d)and (8 e). Inhibitor molecules adsorbed on active sites of Al an a smoother surface was observed when compared to the surface treated with uninhibited alkaline chloride solution.

3. Results and discussion

3.1 Polarization curves

Figure (1) showed the anodic and cathodic polarization curves of 2024 aluminium alloy in alkaline solution (pH=13) of $0.6 \text{ mol dm}^{-3} \text{ NaCl}$ (3.5% W.W NaCl) at four temperatures in the range (293-308)K.

Tafel extrapolation method was used to calculate the corrosion parameters (E_{corr}), (i_{corr}) (b_c) and (b_a) from the polarization curves.

The resetting data were displayed in Table (2) and these data show that corrosion current density (i_{corr}) increases with the increase of temperature, the corrosion potential (E_{corr}) nearly become more negative with the increase of temperature. Anodic and cathodic slopes shows variation in their values which can be attributed to the variation of the rate determining step (r.d.s) of the alloy dissolution reaction (Anodic) and the cathodic reaction involving hydrogen evolution produced by a partial cathodic reaction (reduction) of water. In view of the experimental observation, a tentative corrosion mechanism based on the electrochemical processes for dissolution of aluminium in NaOH may be suggested.

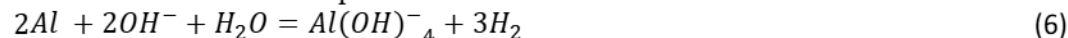
This mechanism can be illustrated by anodic equations (1-4) and cathodic reaction equation(5) respectively for the anode process[8].



and, for the cathode process,



The overall electrochemical process is:



The dissolution of Al metal in the anodic reaction is accompanied by the cathodic reaction which consumes the electrons release in the anodic process in order to form hydrogen atoms which react by combining with other adsorbed hydrogen atom to give bubbles of H_2 gas molecules at the metal surface



3.2 Corrosion activation parameters

Arrhenius suggested the famous equation that correlates the temperature variation with rate of corrosion of 2024 Al alloy which is expressed by (i_{corr}) at a given concentration as[9]

$$\ln(i_{corr}) = \ln A - \frac{E^*}{RT} \quad (8)$$

Here, A is frequency factor, E^* is the activation energy, R is the gas constant and T is the absolute temperature. Equation(8) predicts that plotting of $\ln(i_{corr})$ versus $\frac{1}{T}$ should be linear as we experimentally observed as in Figure(2).

The slope of the line gives $= \frac{-E^*}{RT}$, whereas the intercept of the line extrapolated to $\frac{1}{T} = 0$ gives $\ln A$. the value of activation energy equals to 17.5 kJ mol^{-1} and $A = 19046398 \times 10^{23} \text{ molecule cm}^{-2} \text{ s}^{-1}$ (Table 3).

Entropy of activation (ΔS^*) was calculated from the value of A using the relationship[10].

$$A = \frac{KT^*}{h} \exp \frac{(\Delta S^*)}{R} \quad (9)$$

Where K is Boltzmann constant, h is Plank constant, and T is the temperature of the solution. The value of the entropy of activation was found to be $= -123.5 JK^{-1}.mol^{-1}$ the negative value of ΔS^* for 2024 Al alloy corrosion implies a loss in the overall degree of freedom throughout the formation of the activated complex (association rather than dissociation) for the reaction of 2024 Al alloy constituent with the negative species (Cl^- & OH) leading to the formation of corrosion products, when the activated complex results[11].

3.3. Corrosion inhibition of 2024 Al alloy by amino acids

Figures (3,4) and (5) showed typical polarization curve of 2024 Al alloy in $0.6 mol dm^{-3} NaCl$ solution (pH=13) containing three different concentrations of the amino acids (methionine, glutamic and lysine) separately as green inhibitors over the temperature range (293-308)K. Table (4-6) presents the polarization data E_{corr} and i_{corr} and from these data it can be noticed that the addition of the amino acid caused a decrease in corrosion current densities of 2024 Al alloy and the inhibition effect of each amino acid increases as the concentration of the inhibitor increased in the range $(10^{-3}-10^{-2}) mol dm^{-3}$ at all temperatures of study.

Table (5-6) shows the values inhibition efficiencies (IE%) which could be calculated from equation[13].

$$IE\% = \frac{i_{corr} - i_{corr}}{i_{corr}} \quad (10)$$

Where, i_{corr} and i_{corr} are corrosion current densities in absence and presence of the inhibitor respectively. A maximum value of efficiency was found to be $= 80.4$ at $293 K$ and 10^{-2} conc.

The activation parameters such as E^* and ΔS^* in the range of the studied temperatures (293-308)K for corrosion inhibition of 2024 Al alloy in $0.6 mol dm^{-3} NaCl$ solution in the presence of various concentrations of amino acids, methionine, glutamic acid and lysine separately were calculated from the well-known Arrhenius equation

$$(i_{corr}) = A \exp \left(- \frac{E^*}{RT} \right) \quad (11)$$

The calculated values E^* and ΔS^* are summarized in Table (7). In the presence of each amino acid separately, an increase in E^* values was observed this increase in E^* values in the presence of the inhibitor can be illustrated as follows^[12]: higher values of E^* were found in the presence of inhibitor than those without inhibitor, i.e. the addition of inhibitor raises the energy barrier for the corrosion process emphasizing the electrostatic character of the inhibitors adsorption on 2024 Al alloy surface.

The entropy of activation ΔS^* values are negative in the presence of inhibitor implying the rate determining step for the activated complex is the association rather than the dissociation step. In the presence of the inhibitor ΔS^* moves in the direction of negative values Table (7) which implies the adsorption process is accompanied by a decrease in entropy which is the driving force for the adsorption of inhibitor onto 2042 Al alloy surface[13].

3.4. Thermodynamic parameters of the adsorption isotherms

Adsorption isotherms provide basic information on the nature of interaction between the inhibitor and 2024 Al alloy through applying some adsorption isotherm models. Two main types of interaction can describe the adsorption of inhibitors on the metal surface; they are

physisorption and chemisorption, depending on the chemical structure of the inhibitor, the type of the corrosive medium, and the charge and nature of corrosive metal.

In aqueous solutions, the metal surface is always covered with adsorbed water molecules. Therefore, the adsorption of the inhibitor molecules from an aqueous solution is a quasistatistical process [8], and the inhibitors that have the ability to be adsorbed strongly on the metal surface will hinder the dissolution reaction of the immersed metal into the corrosive medium. The mechanism of corrosion inhibition can be explained in terms of the adsorption behavior based on the calculated coverage degree [14].

The surface coverage Table (7) and the concentrations of inhibitor (amino acids) were tested by fitting to various isotherms like, Langmuir, Temkin and Freundlich. However, the best fit was obtained with Langmuir isotherm as shown in Figure (6) which is given by the following equation [12].

$$\frac{C_{inh}}{\theta} = \frac{1}{K_{ads}} + C_{inh} \quad (12)$$

Where, K_{ads} is the equilibrium constant of the adsorption / desorption processes, and it reflects the affinity of the inhibitor molecules towards surface adsorption sites.

From the intercepts of the straight lines on the C_{inh} / θ axis Figure (6) leads to the equilibrium constant of the adsorption / desorption of amino acid process Table (8). The high value of K_{ads} reveals that the acid molecule possesses strong adsorption onto 2024 alloy surface.

However, K_{ads} decreased with an increase of temperature indicating that adsorption of amino acid onto alloy surface was favorable at lower temperatures.

The equilibrium constant of the adsorption/desorption (K_{ads}) was related to the standard free energy of adsorption according to equation [15].

$$\Delta G^\circ = -RT \ln(55.5 K_{ads}) \quad (13)$$

Where, R is the universal gas constant, T is the absolute temperature, and value 55.5 is the concentration of water in solution.

The standard free energy of adsorption was calculated and given in Table (8). Generally the values of $\Delta G^\circ \cong 26 - 28 \text{ KJ mol}^{-1}$ or less negative are associated with an electrostatic interaction between charged metal surface or more negative involves charge sharing or transfer from the inhibitor molecules to the metal surface to form a co-ordinate covalent bond. So it can be concluded that adsorption of amino acid onto 2024 Al alloy surface takes place through both physical and chemical adsorption [16].

It is generally accepted that the first step in the adsorption of amino acid on the alloy surface usually involves the replacement of one or more water molecules adsorbed on the alloy surface.



$AA \equiv \text{Amino Acid}$

The inhibitor amino acid may then combine with freshly generated metal ions (Al^{+3} or other metal elements in the alloy). On the 2024 AR alloy surface forming metal inhibitor complex [17].



Valuable information about the mechanism of corrosion inhibition can be provided by the values of thermodynamic parameters for the adsorption of the inhibitor.

Thermodynamically, ΔG°_{ads} were related to the standard enthalpy ΔH°_{ads} and standard entropy ΔS°_{ads} according to [18].

$$\Delta G^{\circ}_{ads} = \Delta H^{\circ}_{ads} - T\Delta S^{\circ}_{ads} \quad (17)$$

And the standard enthalpy of adsorption can be calculated on basis of the van't Hoff formula,

$$\ln k_{ads} = -\frac{\Delta H^{\circ}_{ads}}{RT} + constant \quad (18)$$

A plot of $\ln k_{ads}$ versus $\frac{1}{T}$ gives a straight line as shown in Figure (7) . The slope of the straight line is equal to $-\frac{\Delta H^{\circ}_{ads}}{RT}$ the negative values of ΔH° reveals that the adsorption of inhibitor molecules is an exothermic process (for methionine and lysine) and endothermic for glutamic acid. Generally an exothermic adsorption process suggests either physisorption or chemisorption while endothermic process is attributed to chemisorption. The unshared electron pairs in investigated molecules may interact with d-orbitals of Al alloy to provide a protective chemisorbed film[19].

The values of ΔC°_{ads} in the presence of the inhibitor are negative that is accompanied with exothermic adsorption process. ΔS°_{ads} of inhibition process can be calculated from equation(19). According to[18].

$$\Delta S^{\circ}_{ads} = \frac{\Delta H^{\circ}_{ads} - \Delta G^{\circ}_{ads}}{T} \quad (19)$$

References

1. Sainsbury, E.E. and Buchanan, R.A. (2000), "Fundamentals of electrochemical corrosion", ASM International Materials Park, USA.
2. Christia vargel (2004), "Corrosion of Aluminum", Elsevier ltd, new York.
3. Ating, E.I.; Umoren, S.A.; Udousoro, I.I; Ebenso, EE. and Udoh, A.P. (2010), "leaves extract of Ananas sativum as green corrosion inhibitor for aluminium in hydrochloric acid solution", green Chemical let rev. 3, 61-68.
4. Nnanna, L.A.; Anozie, I.U.; voaja, A.G.I. and Akoma, C.S., (2011) "comparative study of corrosion inhibition of aluminium alloy of type AA 3003 in acidic and alkaline media by Euphorbia hirta extract" Afr.J. pur Appl. Chem. 5, 265-271.
5. Obi-Egbed, N.O.; Obot, and Umoren, S.A. (2012) "Spondias mombin L.as a green corrosion inhibitor for aluminium in sulphuric acid: correlation between inhibitive effect and electronic properties of extracts major constituents using density functional theory", Arabain Journal of chemistry 5, 361-373.
6. Deepa prabhu, padmalatha and Roo, (2013), "Corrosion Inhibitor of 6063 aluminium alloy by carianthrum sativum L.seed extract in phosphoric acid medium". J. mater. Environ. Sci, 4, 732-742.
7. Founds, A. S.; Ahmed Abdel nazzar and Ashour, E.A (2011), "Amino acids as environmentally-friendly corrosion inhibitors for CuNi alloy in sulfide-polluted salt water", ZASTIA MATERI JALA 52 broj 1.
8. Refat Hassan, ishaq zaafarany, Adil Gobouri and Hideo takagi, (2013), "ARevisit to the corrosion Inhibitor of Aluminium in Aqueous Alkaline solutions by vilater – soluble Alginates and pectates As Anionic Polyelectrolyte inhibitors", Int. J. of corros, Article under press.
9. Ladler, K.I., (1963), "Reaction kinetics", vol.1, pergmon Aess, new york, NY, USA 1st edition.
10. Glasstone, S.; laidler, K.I.; and Eyring ,H. (1941) "the theory of rate process", Mc Graw. Hill NewYork, NYUSA,.
11. Sinko,P.J.,(2000),"Physical chemical and biopharmaceuticals principles in pharmaceutical science", 5th edition USA, p.413.
12. Scendo, M.; radek, N.; and trela, J., (2012). "Corosion Inhibition of carbon steel in Acid chloride solution Schiff base of N-(2-chlorobenzylidene -4- acetylanline)", Coros. rev. 30-33.
13. Tabi, F.EL.; Fouda, A.S., and Radwan, M.S., (2011), "Inhibitive effect of some thiazazole derivatives on steel corrosion in neutral sodium hydroxide solution". Mater. chem. Phys. 26, 125.
14. Keles, H.; keles, M. ;Dehri I. and serinday, O. (2008) "Adsorption and inhibitor properties of amino phenyl and its schiff base on mild steel corrosion in 0.5 M HCl medium", colloids and surfaces A, 320, no 1-3 pp 138-145.
15. Amin, M.A.; Ibrahim, M.A., (2011) "thiaziazoles as corrosion inhibitors for carbon steel in H_2SO_4 solution", Corros, sci. 53, 873.
16. Ahmad, I.;Prasd, R., and Quraishi A.M., (2010), "Inhibition of mild steel corrosion in acid solution by pheniramine durg, Experimental and theoretical study", corros . Sci 52, 3033.
17. Deny, S.; X. L I H. Fu (2011), "A dsorption and inhibitive action of erhanal extracts chlomolaena adoratal for the corrosion of mild steel in H_2SO_4 solution", Corros. Sci. 53, 822.
18. Murguleseu, L.G., and Rodovie, O., (1961), " metal corrosion", int. conger 10-15 April , London p.202-205.
19. Fouda, A.S.; Hassan, A.F.; Elmorsi, M.A; Fayed, T.A. and Abdelhakim, A., (2014). "Chalcones as environmentally. Friendly corrosion inhibition for SS Type 304 in IM HCL solution" Int. J. EElectrochem. Sci, q.pp 1298-1320.

Table (1): The chemical composition of aluminium Alloy 2024

Si	Fe	Cu	Mn	Mg	Cr	Ni	Zn	V
0.099	0.26	4.46	0.58	1.43	0.01	0.01	0.06	0.016

Table (2): Data of polarization curve of corrosion of aluminium alloy 2024 in 0.6 mol. dm⁻³ NaCl solution at pH (13) over the temperature range (293-308)K

T/K	i_{corr} $\mu\text{A. cm}^{-2}$	$-E_{corr}/\text{mV}$	$b_c/\text{mv. decade}^{-1}$	$b_a/\text{mv. decade}^{-1}$	weight loss $\text{g. m}^{-2}.\text{day}^{-1}$	Penetration loss/ mm. year^{-1}
293	1750	1320	162.6	573.7	141	19.1
298	2510	1347	179.2	378.3	202	27.3
303	2670	1359	122.8	310.9	216	29.1
308	3490	1320	210.5	379.6	281	38

Table (3): Activation energy E_a , pre exponential (A) and entropy of activation (ΔS^*) for aluminium alloy 2024 corrosion in Solution in pH=13.

E_a K. J. mol ⁻¹	$-\Delta S^*$ J. K ⁻¹ . mol ⁻¹	A/molecule cm ⁻² S ⁻¹
17.5	123.5	19046398×10^{23}

Table (4): Values of (E_{corr} , i_{corr}) and inhibitors effeciienly concentrations of methionine at temperature range (293-300) in pH=13.

T/K	Inhibition conc. mol. dm^{-3}	E_{corr}/mV	$i_{corr}/\text{mA. cm}^{-2}$	θ	IE % from i_{corr}
293	0	1320	1750	-	-
	1×10^{-3}	1348.5	548	0.69	69
	5×10^{-3}	1346	469	0.73	73
	1×10^{-2}	1300	367	0.79	79.1
298	0	1347	2500	-	-
	1×10^{-3}	1352	799	0.68	68
	5×10^{-3}	1347	707	0.71	71.7
	1×10^{-2}	1339	459	0.78	78.1
303	0	1359	2670	-	-
	1×10^{-3}	1340	897	0.67	67
	5×10^{-3}	1340	835	0.69	69
	1×10^{-2}	1316	716	0.73	73.3
308	0	1320	3490	-	-
	1×10^{-3}	1335	1220	0.65	65.1
	5×10^{-3}	1436.5	1200	0.66	66
	1×10^{-2}	1301	986	0.71	71.8

Table (5): Values of (E_{corr} , i_{corr}) and inhibitors efficiency concentrations of Lysine at temperature range (293-308) in pH=13.

T/K	Inhibition conc. mol. dm ⁻³	E_{corr} /mv	i_{corr} /mA. cm ⁻²	θ	IE % from i_{corr}
293	0	1320	1750	-	-
	1×10^{-3}	1344	489	0.72	72.1
	5×10^{-3}	1366	473	0.73	73
	1×10^{-2}	1347	451	0.74	74.3
298	0	1347	2500	-	-
	1×10^{-3}	1325	718	0.713	71.3
	5×10^{-3}	1327	696	0.72	72.2
	1×10^{-2}	1354	688	0.725	75.5
303	0	1290	2670	-	-
	1×10^{-3}	1290	801	0.70	70.2
	5×10^{-3}	1293	770	0.71	71
	1×10^{-2}	1275	765	0.715	71.5
308	0	1320	3490	-	-
	1×10^{-3}	1295	1100	0.685	68.5
	5×10^{-3}	1290	1070	0.69	69
	1×10^{-2}	1287	1040	0.714	71.4

Table (6): Values of (E_{corr} , i_{corr}) and inhibitors efficiency percent concentrations of Glutamic acid at temperature range (293-308) in pH=13.

T/K	Inhibition conc. mol. dm ⁻³	E_{corr} /mv	i_{corr} /mA. cm ⁻²	θ	IE % from i_{corr}
293	0	1320	1750	-	-
	1×10^{-3}	1328	480	0.73	72.6
	5×10^{-3}	1300	460	0.74	73.4
	1×10^{-2}	1336	344	0.804	80.4
298	0	1347	2500	-	-
	1×10^{-3}	1296	701	0.72	72
	5×10^{-3}	1419	658	0.737	73.7
	1×10^{-2}	1287	519	0.79	79.4
303	0	1359	2670	-	-
	1×10^{-3}	1318	780	0.71	71
	5×10^{-3}	1321	723	0.73	73.1
	1×10^{-2}	1302	635	0.76	76.4
308	0	1320	3490	-	-
	1×10^{-3}	1286	1030	0.705	70.5
	5×10^{-3}	1289	949	0.729	72.9
	1×10^{-2}	1269	870	0.75	75.1

Table (7): Activation energy E_a , pre exponential (A) and entropy of activation (ΔS^*) for the corrosion of AA 2024 in pH = 13 in 0.6 mol. dm⁻³ NaCl solution and different concentration of L-methionine, L-glutamic acid L-lysine.

Inhibition	conc. of inhibition mol. dm ⁻³	E_a /KJ . mol ⁻¹	$-\Delta S^*$ J. K. mol ⁻¹	A/ molecule cm ⁻² . S ⁻¹
L-meth	1×10^{-3}	30.4	95	602300000×10^{23}
	5×10^{-3}	37.72	66.69	$18612849390 \times 10^{23}$
	1×10^{-2}	44	47.88	$181891692100 \times 10^{23}$
L-glu	1×10^{-3}	34.2	78.72	$4333241195 \times 10^{23}$
	5×10^{-3}	38	57.38	$57519203460 \times 10^{23}$
	1×10^{-2}	46.74	39.9	$478423895800 \times 10^{23}$
L-lys	1×10^{-3}	34.77	77.14	$5245813702 \times 10^{23}$
	5×10^{-3}	38	65.93	$19046398350 \times 10^{23}$
	1×10^{-2}	40.47	58.9	$47842389580 \times 10^{23}$

Table (8): Equilibrium constant adsorption/desorption standard free energy enthalpy and entropy of adsorption onto AA 2024 in 0.6 mol. dm⁻³ NaCl solution in pH = 13 in the presence of three amino acids L-methionine, L-glutamic acid L-lysine.

Inhibition	T/K	K_{ads} . mol ⁻¹	ΔG_{ads} *J. K. mol ⁻¹	ΔH_{ads} *J. K. mol ⁻¹	$\frac{\Delta H_{ads}}{J. K. mol^{-1}. K^{-1}}$
L-methionine	293	2500	28.8	-94.62	42.1
	298	1250	27.6		41.0
	303	026	28.3		39.9
	308	384	25.5		39.0
L-glutamic acid	293	2500	28.79	28.19	20
	298	2000	28.73		18
	303	1666	28.67		16
	308	1428	28.12		3.0
L-lysine	293	909	26.34	-15.90	36.0
	298	769	26.22		34.6
	303	714	26.61		35.3
	308	666	26.84		35.5

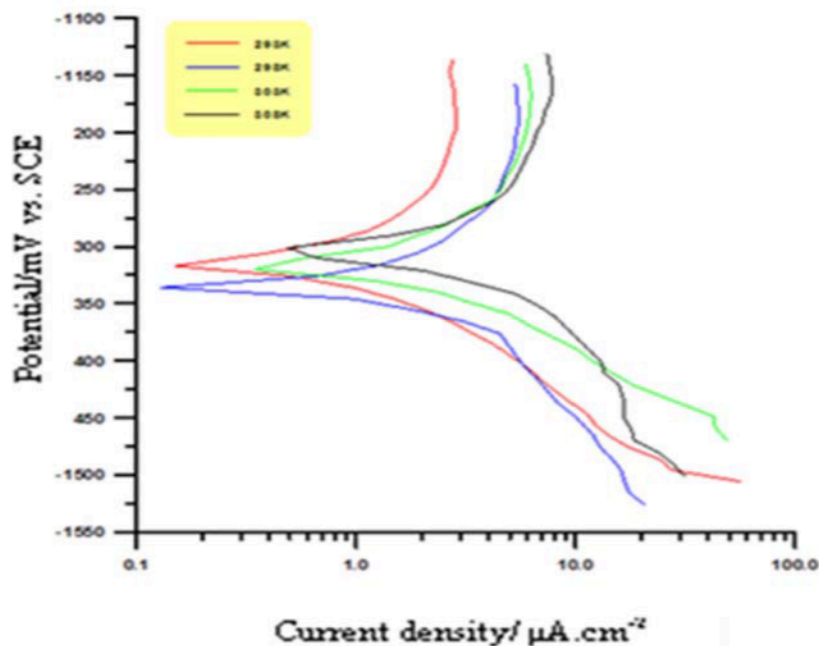
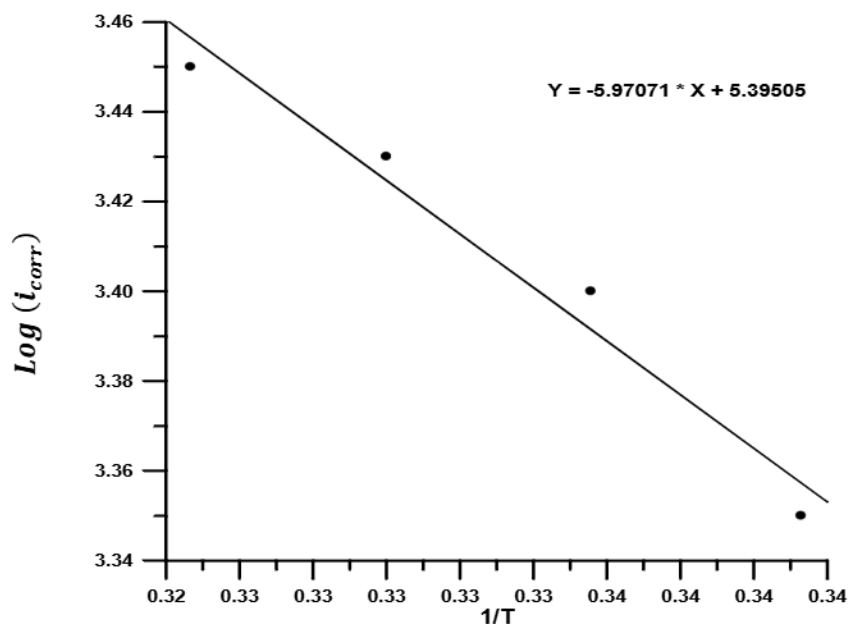


Figure (1): Polarization curves of 2024 AA corrosion pH=13 with 0.6 mol. dm⁻³ NaCl solution at four temperatures in the range of (293-308)K.



Figure(2): Arrhenius Plot relating Log (i_{corr}) to $1/T$ for the 2024 AA corrosion pH=13 with 0.6 mol. dm⁻³ NaCl solution at four temperatures in the range of (293-308)K.

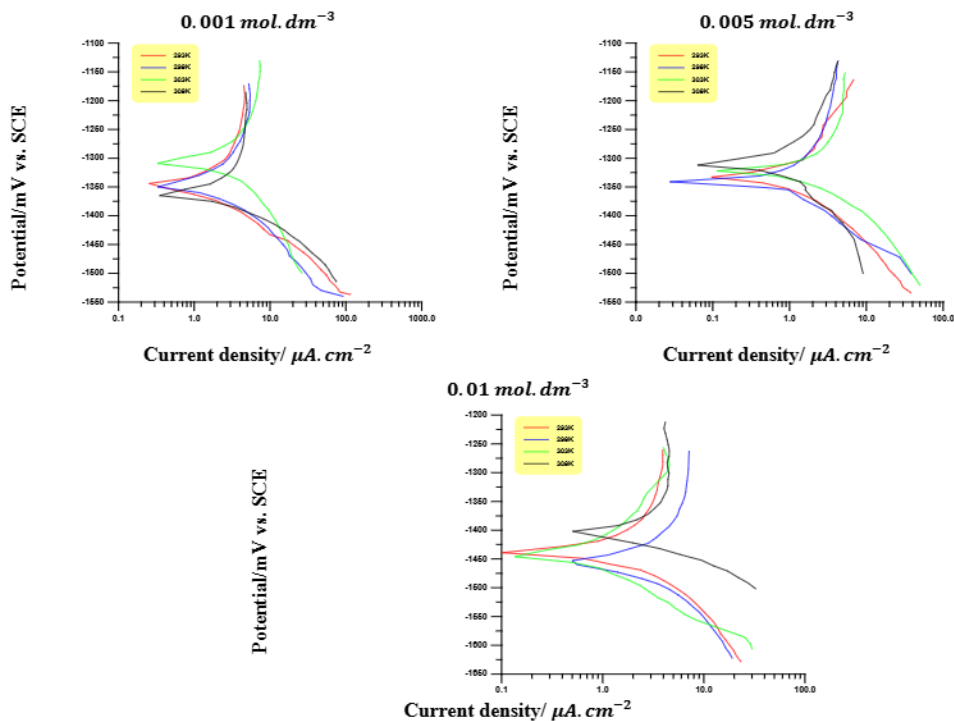


Figure (3): Polarization curves of 2024 AA corrosion in 0.6 mol. dm⁻³ NaCl solution in pH=13 over the temperature range (293-308)K with three concentration of L-methionine (10⁻³, 5 × 10⁻³ and 1 × 10⁻² mol. dm⁻³)

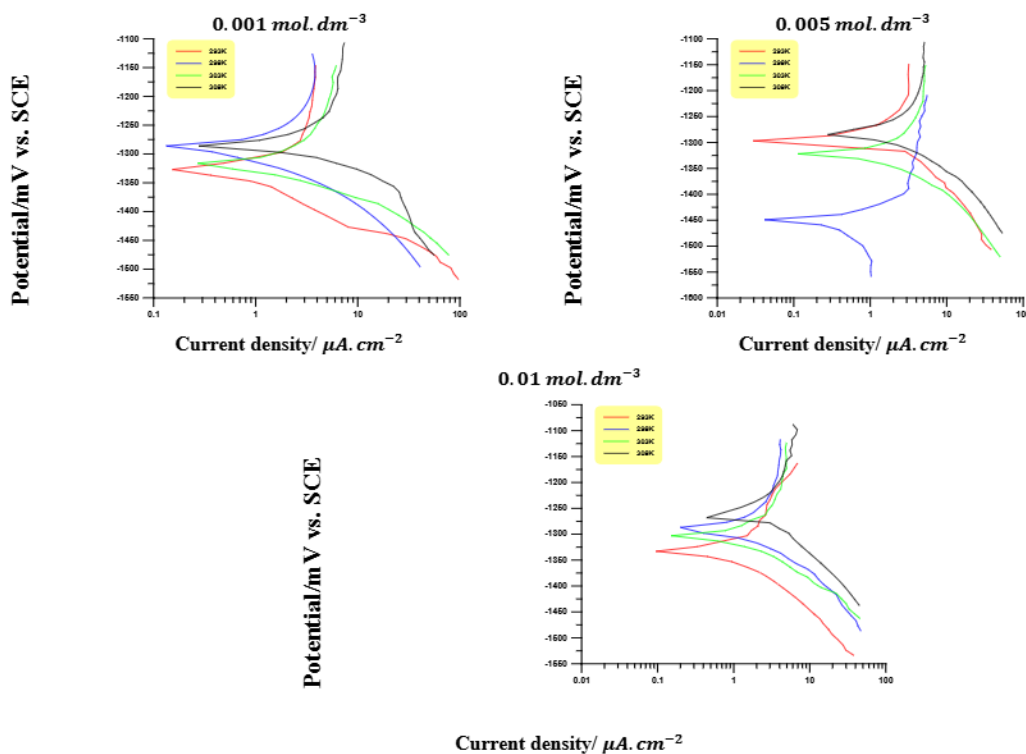


Figure (4): Polarization curves of 2024 AA corrosion in 0.6 mol. dm⁻³ NaCl solution in pH=13 over the temperature range (293-308)K with three concentrations of L-Glutamic acid (10⁻³, 5 × 10⁻³ and 1 × 10⁻² mol. dm⁻³)

0.001 mol. dm⁻³0.005 mol. dm⁻³

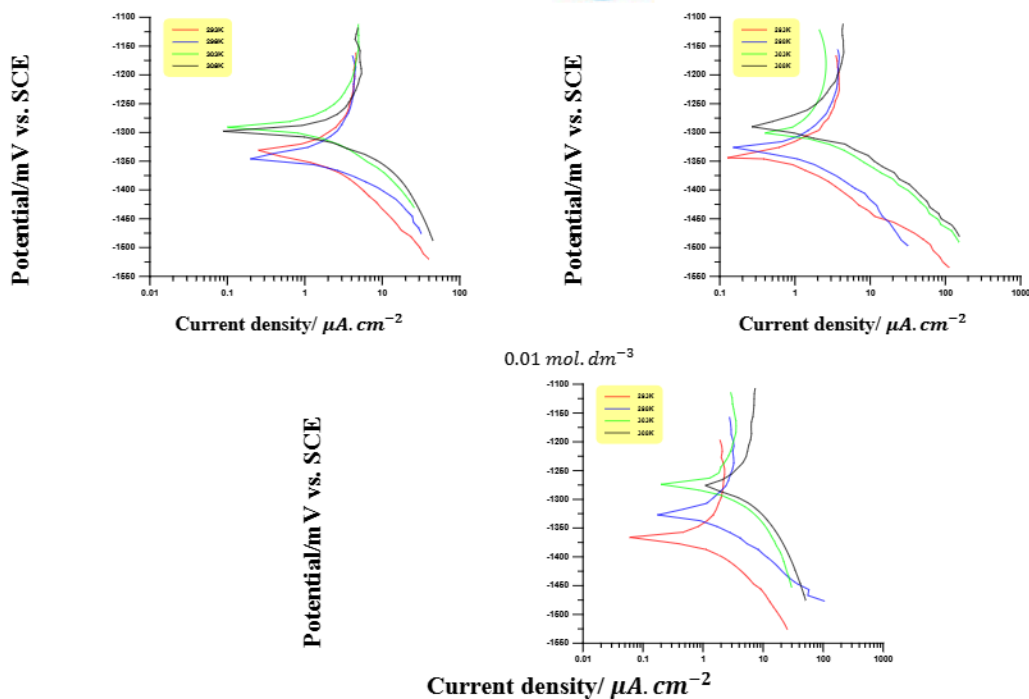


Figure (5): Polarization curves of 2024 AA corrosion in 0.6 mol. dm^{-3} NaCl solution in pH=13 over the temperature range (293-308)K with three concentrations of L-lysine (10^{-3} , 5×10^{-3} and $1 \times 10^{-2} \text{ mol. dm}^{-3}$)

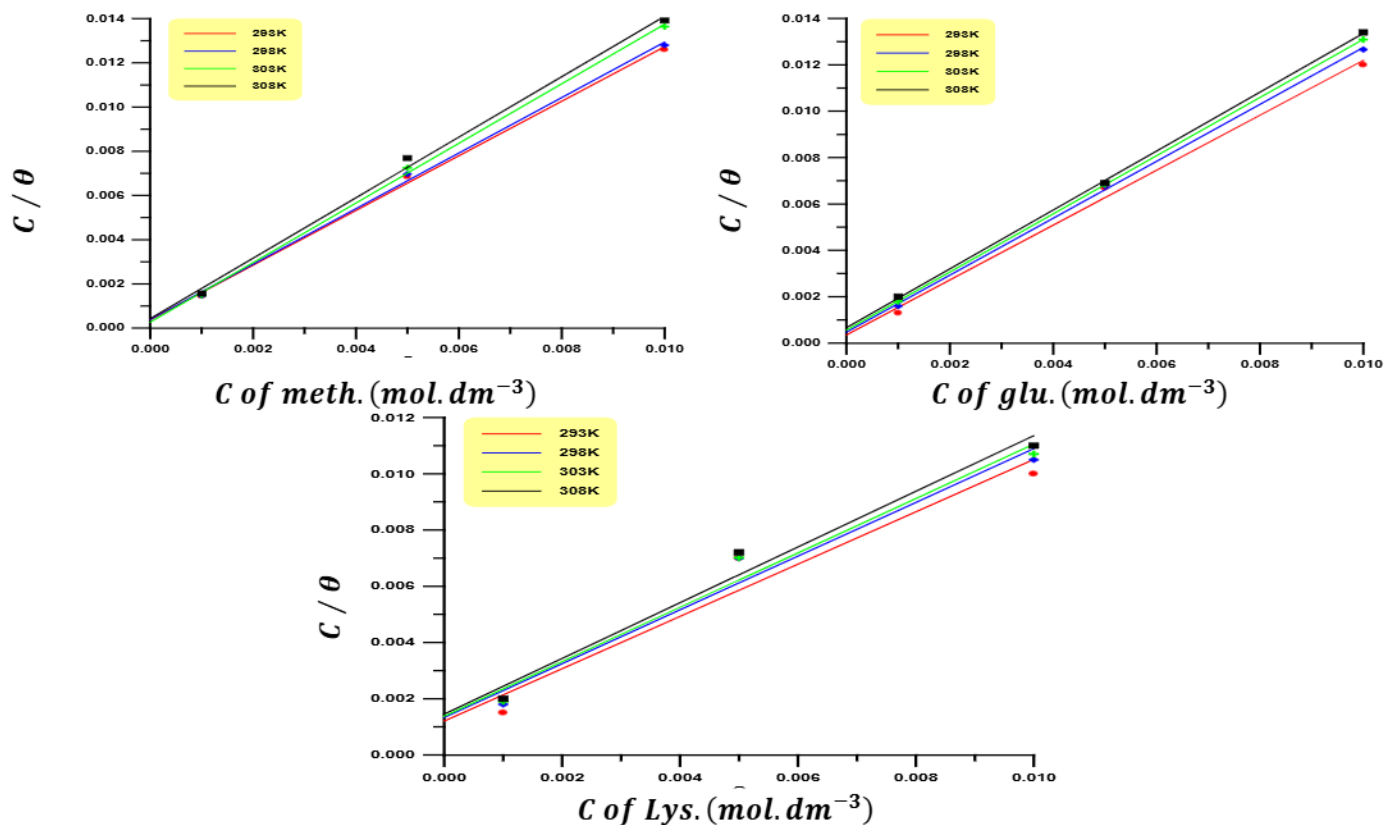


Figure (6): Langmuir adsorption plots of three amino acid onto 2024AA in $(0.6 \text{ mol. dm}^{-3})$ NaCl solution of various temperatures at pH value (pH=13)

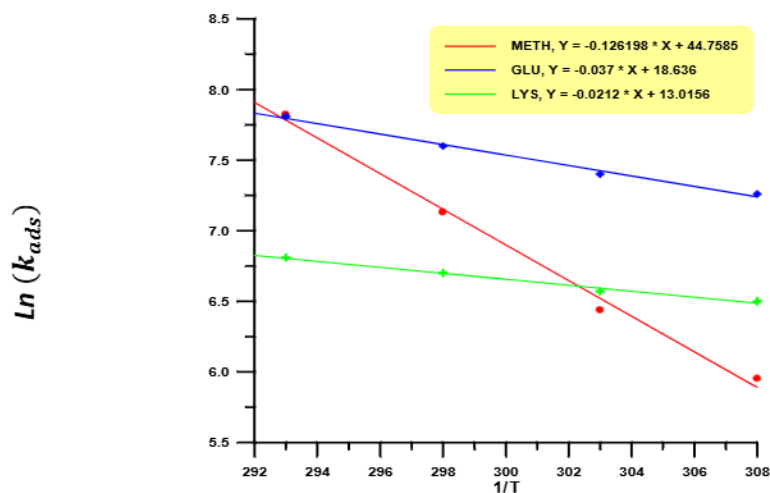
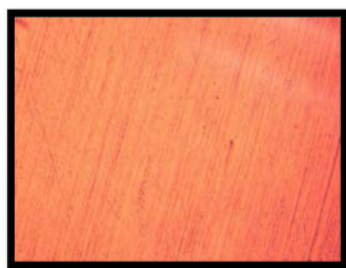
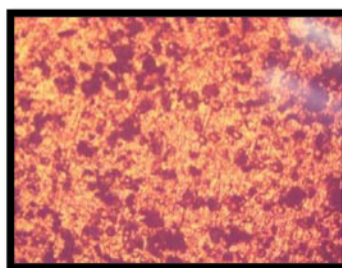


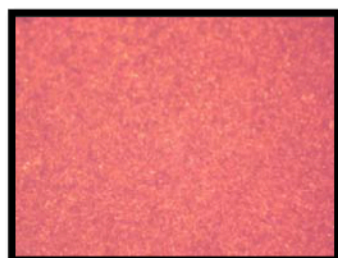
Figure (7): Van't Hoff plot of 2024AA in $(0.6 \text{ mol. dm}^{-3})$ NaCl solution containing three amino acids of various temperatures at pH value (13)



a. Polished 2024 AA



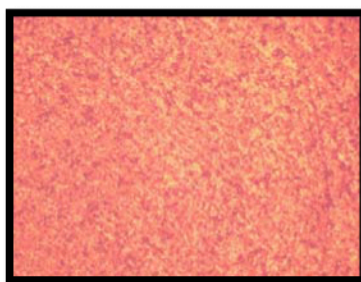
b. After immersion in the corrosive medium



c. After immersion in the corrosive medium + L-methionine



d. After immersion in the corrosive medium + L-Glutamic acid



e. After immersion in the corrosive medium + L-lysine

Figure (8): Optical microscope micrographs of 2024AA surface in pH=13.

الاحماض الامينية كمتبطات صديقة للبيئة لتآكل سبيكة الالمنيوم 2024 في المحيط القاعدي

وصال عبد العزيز عيسى

زينب وجدي احمد

قسم الكيمياء / كلية التربية للعلوم الصرفة (ابن الهيثم) / جامعة بغداد

استلم في: 24/مارس/2015، قبل في: 23/حزيران/2015

الخلاصة

يتناول موضوع البحث دراسة كهروكيميائية لسلوك تآكل سبيكة الالمنيوم 2024 في محلول قاعدي ($pH = 13$) لكلوريد الصوديوم بتركيز (0.6 mol. dm^{-3}) بغياب وجود تراكيز مختلفة من الاحماض الامينية الثلاثة (ميثونين وحمض الكلوتاميك واللاسين) كمتبطات صديقة للبيئة على مدى درجات الحرارة K (308 – 293) اشتملت الدراسة على طريقة الاستقطاب الكهروكيميائي باستعمال جهاز المجهاد الساكن والمجهر الضوئي. وجد ان كفاءة التثبيط تزداد بزيادة تركيز المثبط وتقل بزيادة درجة الحرارة. وجد ان اعلى قيمة لكفاءة المثبط وجدت مع اللاسين = 80.4 عند 293K وبتركيز المثبط $0.10^{-2} \text{ mol. dm}^{-3}$. اظهرت النتائج ان التثبيط يحدث من خلال امتزاز جزيئات المثبط على سطح الفلز ووجد انها تتبع مسار درجة الحرارة للانكمير (Langmuir Isotherm for Adsorption) وقد تم حساب بعض المعلومات الثرموديناميكية طاقة جيبس (ΔG_{ads}) وطاقة التنشيط (E_a) لتوضيح ميكانيكية تثبيط التآكل. قياسات الاستقطاب اوضحت بأن المثبط من نوع المختلط المعلمات الحركية حسبت باستعمال نظرية أرينيوس – اقترضت ميكانيكية مناسبة لتآكل سبيكة الالمنيوم 2024 في المحيط القاعدي وقد تم تمييز سطح الفلز قبل وبعد التثبيط باستعمال المجهر الضوئي.

الكلمات المفتاحية: تثبيط التآكل, سبيكة 2024, حوامض امينية, طاقة جيبس الحرة للامتزاز, ميكانيكية الامتزاز .